THE JOURNAL OF BIOLOGICAL CHEMISTRY VOL. 283, NO. 24, pp. 16790–16800, June 13, 2008

Transglutaminase Induces Protofibril-like Amyloid β-Protein Assemblies That Are Protease-resistant and Inhibit Long-term Potentiation*[S]

Received for publication, March 20, 2008 Published, JBC Papers in Press, April 8, 2008, DOI 10.1074/jbc.M802215200

Dean M. Hartley[‡1], Chaohui Zhao[‡], Austin C. Speier[§], Gavitt A. Woodard[§], Shaomin Li[¶], Zongli Li[¶], and Thomas Walz[¶]

From the [‡]Department of Neurological Sciences, Rush University Medical Center, Chicago, Illinois 60612, [§]Harvard College, Faculty of Arts and Sciences, Harvard University, Cambridge, Massachusetts 02138 and the [¶]Departments of Neurology and Cell Biology, Harvard Medical School, Boston, Massachusetts 02115

An increasing body of evidence suggests that soluble assemblies of amyloid β-protein (Aβ) play an important role in the initiation of Alzheimer disease (AD). *In vitro* studies have found that synthetic Aβ can form soluble aggregates through self-assembly, but this process requires Aβ concentrations 100- to 1000-fold greater than physiological levels. Tissue transglutaminase (TGase) has been implicated in neurodegeneration and can cross-link Aβ. Here we show that TGase induces rapid aggregation of Aβ within 0.5–30 min, which was not observed with chemical cross-linkers. Both Aβ40 and Aβ42 are good substrates for TGase but show different aggregation patterns. Guinea pig and human TGase induced similar Aβ aggregation patterns, and oligomerization was observed with Aβ40 concentrations as low as 50 nM. The formed Aβ40 species range from 5 to 6 nm spheres to curvilinear structures of the same width, but up to 100 nm in length, that resemble the previously described self-assembled Aβ protofibrils. TGase-induced Aβ40 assemblies are resistant to a 1-h incubation with either neprilysin or insulin degrading enzyme, whereas the monomer is rapidly degraded by both proteases. In support of these species being pathological, TGase-induced Aβ40 assemblies (100 nM) inhibited long term potentiation recorded in the CA1 region of mouse hippocampus slices. Our data suggest that TGase can contribute to AD by initiating Aβ oligomerization and aggregation at physiological levels, by reducing the clearance of Aβ due to the generation of protease-resistant Aβ species, and by forming Aβ assemblies that inhibit processes involved in memory and learning. Our data suggest that TGase might constitute a specific therapeutic target for slowing or blocking the progression of AD.

Oligomerization and aggregation of the amyloid β-protein (Aβ)[2] are thought to comprise a central mechanism in the initiation and progression of Alzheimer disease (AD). Aβ was first implicated in AD when it was found to be the major protein in amyloid plaques, one of the histopathological hallmarks of AD, in which Aβ exists as fibrils. In support of the involvement of Aβ in AD, early studies investigating the neurotoxicity of Aβ found that longer forms of Aβ (*e.g.* Aβ42) aggregated faster than shorter ones (1) and that aggregation was essential for neurotoxicity (2). For self-aggregation to occur *in vitro*, micromolar Aβ concentrations are required (3). These Aβ concentrations far exceed the physiological levels, even in the AD brain, which are in the low nanomolar range (4–6). This discrepancy suggested that a pure self-assembly mechanism may not account for oligomerization and aggregation *in vivo*.

Tissue transglutaminase (TGase) is a complex protein with multiple functions, including serine kinase activity, G protein signaling, and the catalytic capability to cross-link proteins between lysine and glutamine residues, forming a covalent isodipeptide bond (7). TGase occurs abundantly in the brain and has been implicated in neurodegeneration (8, 9). Aβ contains the necessary lysine and glutamine residues for TGase-catalyzed cross-linking and has previously been shown to be a substrate for TGase (10–12). Thus, TGase may be a likely candidate to play a role in the pathophysiology of AD.

Here we found that TGase induces monomeric Aβ to rapidly form oligomers and aggregates in a time- and concentration-dependent manner. Most importantly, we show that TGase lowers the concentration for Aβ oligomerization so it can occur at physiological Aβ levels and that it induces Aβ species that are resistant to degradation by metalloproteases. Additionally, EM analysis showed that the TGase-induced Aβ assemblies have the same morphologies as the previously described protofibrils that result from self-aggregation (13, 14). The importance of these findings is supported by the ability of the TGase-induced Aβ assemblies to attenuate long term potentiation (LTP), a process thought to be affected in the early stages of AD. Thus,

* This work was supported, in whole or in part, by National Institutes of Health Grant AG19770 (to D. M. H.) from NIA. This work was also supported by the Alzheimer's Association (to D. M. H.) and the Harvard College Research Program and Merck Research Laboratories' Summer Undergraduate Research Fellowship Program (Boston) (to A. S. and G. A. W.). The costs of publication of this article were defrayed in part by the payment of page charges. This article must therefore be hereby marked "*advertisement*" in accordance with 18 U.S.C. Section 1734 solely to indicate this fact.

[S] The on-line version of this article (available at http://www.jbc.org) contains supplemental Fig. S1.

[1] To whom correspondence should be addressed: Dept. of Neurological Sciences, Rush University Medical Center, 1735 W. Harrison St., Rm. 316, Chicago, IL 60612. Tel.: 312-563-3599; Fax: 312-942-7452; E-mail: dean_hartley@rush.edu.

[2] The abbreviations used are: Aβ, amyloid β-protein; EM, electron microscopy; AD, Alzheimer disease; TGase, transglutaminase; LTP, long term potentiation; SEC, size exclusion chromatography; DMS, dimethyl suberimidate; Bis-Tris, 2-[bis(2-hydroxyethyl)amino]-2-(hydroxymethyl)propane-1,3-diol; MES, 4-morpholineethanesulfonic acid; fEPSP, field excitatory postsynaptic potential; G3PD, glyceraldehyde-3-phosphate dehydrogenase; IDE, insulin-degrading enzyme; NEP, neprilysin; ACSF, artificial cerebrospinal fluid.

the TGase-induced oligomerization and aggregation of Aβ provides a mechanism that could explain both the formation and the persistence of pathologically active Aβ species *in vivo*.

EXPERIMENTAL PROCEDURES

Chemicals—Unless noted otherwise, chemicals were purchased from Sigma and Invitrogen. Insulin-degrading enzyme was a gift from Dr. Malcolm Leissring. Human neprilysin was purchased from R&D Systems (Minneapolis, MN), 6E10 antibody from Signet Laboratories (Dedham, MA), and anti-TGase antibody ab2386 from Abcam (Cambridge, MA).

Aβ Peptide Preparation—Lyophilized Aβ peptides were obtained from multiple sources as a trifluoroacetic salt (Biopolymer Facility, Brigham and Women's Hospital, Anaspec, San Jose, CA, California Peptide, Napa, CA). Aβ was prepared for TGase-mediated cross-linking reactions by initially dissolving the peptide in 100% DMSO and then diluting the solution with water and HEPES buffer (final concentration, 232 μM Aβ in 5% DMSO and 25 mM HEPES, pH 7.6).

Size Exclusion Chromatography—Monomeric Aβ was purified, and Aβ assemblies were characterized by size exclusion chromatography (SEC) using either a Superdex 75 or Superose 6 column (10 × 300 mm). The Superdex 75 column was initially used to separate low molecular weight Aβ from protofibrils as previously described (14). The Superose 6 column was used to separate a larger range of Aβ aggregates. For a subset of experiments, Aβ40 (1 mg/ml) was denatured in 6 M guanidine HCl prior to SEC purification. Samples were run at a flow rate of 0.5 ml/min, and protein was monitored at wavelengths of 210 and 280 nm. Both columns were run isocratically using a buffer containing 70 mM NaCl and 5 mM Hepes, pH 7.5.

Protein Assay—The Bradford protein assay (Bio-Rad) was modified by adding a 10-min incubation of the samples in 4 M urea at room temperature, before dye addition.

Thioflavin T Binding—Thioflavin T dye (10 μM) in 100 mM glycine buffer, pH 8.5, was mixed with an equal amount of sample (50 μl of each for 96-well assays), incubated for 10 min at room temperature in the dark, and read out at 446_{ex} and 490_{em} (15).

Cross-linking Reactions—Tissue transglutaminase (TGase, or TGase 2, EC 2.3.2.13) reactions in 70 mM NaCl, 2.5 mM $CaCl_2$, 40 mM HEPES, pH 7.5, 1 mM dithiothreitol were initiated by adding Aβ40. The reactions were incubated for the times and at the temperatures specified for the various experiments. Reactions were stopped either by the addition of EDTA (50 mM final concentration) or the addition of a TGase inhibitor (LDDN-80042, courtesy of Laboratory of Neurodegeneration and Drug Discovery, Brigham and Women's Hospital, Boston) at 10–20 μM. In some experiments the Aβ peptide was concentrated using a 3-kDa cutoff spin filter in the presence of 50 mM EDTA and 0.11 mM SDS. Because Aβ42 has a higher propensity to self-aggregate, the experiments described above were performed with Aβ40 to keep self-aggregation at a minimum, because it might confound the kinetics of TGase-induced aggregation (*i.e.* cross-linking of monomer *versus* cross-linking of pre-formed oligomers or aggregates). Guinea pig TGase purified from liver was purchased from Sigma-Aldrich. Recombinant human TGase expressed in *Escherichia coli* (16, 17) was a gift from Dr. Ross Stein. To allow direct comparison of the ability of human and guinea pig TGase to induce oligomerization of Aβ40, the concentrations of active sites (micromolar) of both enzyme preparations were determined by the Case and Stein (16) method and were found to be 13.5 and 40 μM, respectively. Unless noted otherwise, all experiments were carried out with guinea pig TGase.

The cross-linking reagent dimethyl suberimidate (DMS) was used as described by Davies and Stark (18). Solutions containing glyceraldehyde-3-phosphate dehydrogenase (3 mg/ml), aldolase (5 mg/ml), or Aβ40 (0.43 μg/ml) were incubated with DMS (2 mg/ml) at 30 °C overnight in 0.2 M triethanolamine hydrochloride (pH 8.5).

Gel Electrophoresis and Western Blotting—Samples were boiled (unless noted otherwise) and separated on Bis-Tris 4–12% NuPAGE gels in MES-SDS running buffer (Invitrogen). Proteins were transferred onto an Optitran BA-S 83 0.2-μm supported nitrocellulose membrane (Schleicher and Schuell). Membranes were not boiled before blocking. Membranes were blocked in 5% powdered milk in Tris-buffered saline (20 mM Tris, 137 mM NaCl, and 0.1% Tween 20 (TBST)) for 30 min, probed with the 6E10 (1:5000, Signet) antibody, and developed with a donkey anti-mouse secondary antibody (1:8000) conjugated to horseradish peroxidase (Jackson ImmunoResearch Laboratories). Chemiluminescence substrate (ECL+, GE Healthcare) was used to visualize Aβ bands. Gels not being transferred for Western blotting were stained with SYPRO Red reagent in 10% acetic acid for 1 h to visualize proteins (per manufacturer's instructions, Invitrogen).

Electron Microscopy—Aβ was purified by SEC using the guanidine HCl and Superose 6 column method (see above). A common stock of fresh Aβ was prepared, and aliquots were sampled at various time points for EM analysis. The samples were prepared by conventional negative staining with 0.75% uranyl formate as described previously (19). Reactions were considered to be terminated at the time when excess peptide was washed from the grid, which was ~25 s into the EM grid preparation procedure. Grids were examined with a FEI Tecnai 12 electron microscope operated at an acceleration voltage of 120 kV. Images were recorded at a magnification of 52,000× and a defocus of ~−1.5 μm using a Gatan 2k × 2k charge-coupled device camera.

Protease Degradation—Aggregated Aβ was prepared by mixing Aβ with TGase (see above) and stopped with the TGase inhibitor LDDN-80042 (10 μM). Degradation was evaluated with 50–100 nM protease for different time periods at 37 °C and halted with 1 mM 1,10-phenanthroline. Samples were analyzed by Western blotting using the 6E10 anti-Aβ antibody.

Electrophysiological Recordings—Mouse transverse hippocampal slices were prepared and field excitatory postsynaptic potentials (fEPSP) were recorded in the CA1 region of the hippocampus as described previously (20). To induce LTP, two consecutive trains (1 s) of stimuli at 100 Hz separated by 20 s were applied to the Schaffer collaterals.

Traces were analyzed using the LTP Program (21). The fEPSP magnitude was measured using the initial fEPSP slope, and three consecutive responses (1 min) were averaged and normalized to the mean value recorded 20–30 min into the

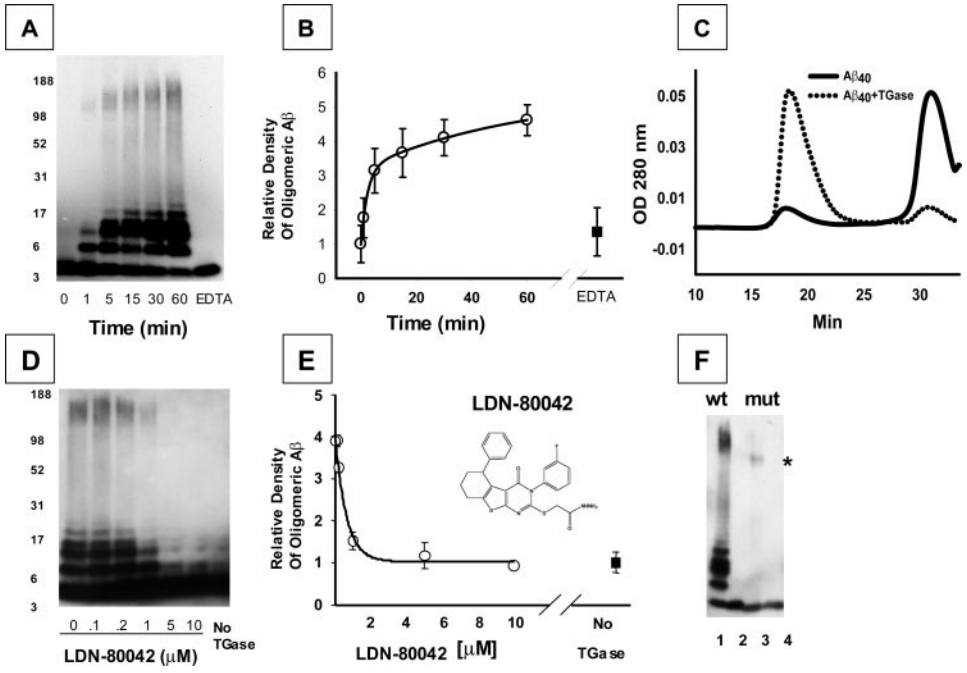

FIGURE 1. **TGase induces Aβ aggregation in a time- and calcium-dependent manner.** *A*, the Western blot analysis shows the time dependence of Aβ40 (25 μM) aggregation induced by TGase at room temperature and stopped with EDTA. In the "*EDTA*" sample, the chelator was added before TGase. *B*, densitometry of Western blots such as the one in *panel A* shows that TGase induces rapid aggregation of Aβ. For the quantification of the immunoblot, the total signal due to oligomerization (>4 kDa) in each lane was measured and normalized to the signal at $T = 0$, which was given a value of 1. Each data point represents the mean of three separate experiments (±S.E.). *C*, a Superdex 75 size exclusion column was used to show the conversion from substrate (low molecular weight Aβ) to product (aggregated Aβ) induced by TGase addition. Aβ40 alone showed little conversion of LWM Aβ (31-min peak) (*solid line*), whereas in the sample containing TGase the majority of Aβ was converted into aggregates (19-min peak) (*dotted line*). *D*, the TGase inhibitor LDDN-80042 was highly effective in attenuating the aggregation of Aβ40, blocking aggregation at concentrations ranging from 0.1 to 10 μM. The "*No TGase*" sample was run under identical conditions, but without TGase. *E*, densitometry of Western blots such as the one in *panel D* shows TGase inhibition with LDDN-80042. For this analysis, the signal from the bands at 8 kDa and higher were measured and normalized against the signal from the same area measured in the sample lacking TGase, which was given a value of 1 ($n = 3$, ±S.E.). *F*, a mutant Aβ40 peptide (*i.e.* Aβ40 with its two lysines mutated to alanine = *mut*) did not form aggregates in the presence of TGase (*lane 1*, Aβ40 + TGase; *lane 2*, Aβ40 only; *lane 3*, mutant Aβ40 + TGase; *lane 4*, mutant Aβ40 only). The *asterisk* indicates Aβ40 bound to TGase.

baseline recording, but before tetanus application. Data were pooled across animals of the same age and are presented as mean ± S.E. LTP was evaluated by measuring fEPSPs 60 min after the tetanus application. The following statistical analysis was carried out: the same time window samples of the control and drug administrations were compared using paired, two-tailed Student's *t* test. In the case of multiple comparisons, samples were analyzed by one-way analysis of variance. Student-Newman-Keuls post-hoc tests were used to examine the significance of multiple pairwise comparisons.

RESULTS

Amyloid-β protein (Aβ) undergoes self-aggregation *in vitro* above a critical concentration, which has been reported as 5–100 μM depending on whether Aβ40 or Aβ42 was used (22, 23). This process requires hours to days to occur, although aggregation can be accelerated with higher concentrations of Aβ. Physiological concentrations of Aβ are significantly lower, in the pico- to nanomolar range, posing the conundrum as to what *in vivo* factors allow Aβ to oligomerize or aggregate at lower concentrations. Our experiments show that TGase causes rapid, time-dependent oligomerization of Aβ40. TGase (6.25×10^{-3} units/ml) was added to an Aβ40 solution (25 μM) at room temperature, aliquots were taken at 0, 1, 5, 15, 30, and 60 min, and the reaction was stopped with EDTA. The aliquots were resolved on an SDS-PAGE gel, illustrating the rapid kinetics of the TGase-induced oligomerization of Aβ (Fig. 1*A*). This rapid assembly appears as a laddering of Aβ that represents the incremental addition of Aβ monomers into oligomers that develop into larger assemblies and eventually grow too large to enter the gel. This time-course experiment shows that TGase induces rapid oligomerization of Aβ under these specific conditions, reaching ~50% activity in 5 min (Fig. 1*B*). TGase activity was inhibited in the presence of the calcium chelator EDTA (5 mM) (Fig. 1, *A* and *B*). It is important to point out that self-assembled Aβ are SDS-labile, particularly at elevated temperatures. Boiling the reaction products of self-assembled Aβ briefly prior to electrophoresis dissociates most of the self-aggregated Aβ species (data not shown). By contrast, Aβ species formed in the presence of TGase remain intact upon boiling.

The oligomerization of Aβ by TGase can be observed by SEC as the substrate-to-product ratio. At time 0 most of Aβ40 is in a low molecular weight form (predominantly monomeric Aβ40) and elutes at 31 min, but after a 30-min incubation with TGase, Aβ40 is converted into larger assemblies as observed by an increase in the void peak that elutes at 17 min (Fig. 1*C*, *dotted line*). In contrast, Aβ40 incubated for 30 min without TGase shows little conversion of the low molecular weight Aβ40 peak into larger assemblies (Fig. 1*C*, *solid line*). In support of TGase being responsible for the fast Aβ oligomerization kinetics, addition of the recently developed TGase inhibitor LDDN-80042 (24) at a concentration of 2.5 μM resulted in almost complete inhibition of Aβ oligomerization (Fig. 1, *D* and *E*). Additional support for TGase driving this process is the lack of aggregation observed with a mutant Aβ40 peptide. Wild-type Aβ40 showed rapid assembly formation in the presence (Fig. 1*F*, *lane 1*) but not in the absence of TGase (Fig. 1*F*, *lane 2*). To show the specificity of this reaction, the two lysine residues in Aβ40 were mutated to alanine, because TGase requires a lysine for the formation of an ε-(γ-glutamyl)lysine isopeptide bond (7). Little to no oligomerization was observed with the mutant Aβ40 irrespective of the presence (Fig. 1*F*, *lane 3*) or absence of TGase (Fig. 1*F*, *lane 4*). Interestingly, the single remaining cross-link site, a glutamine

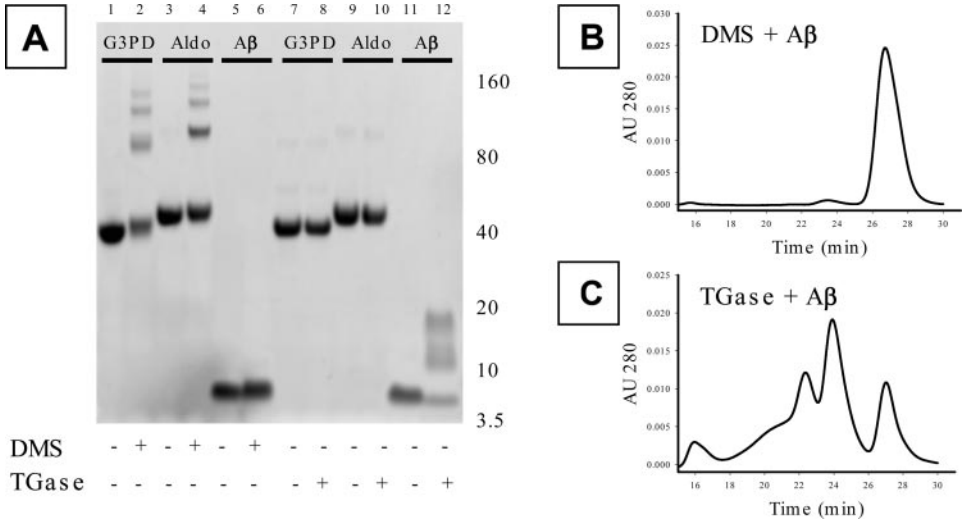

FIGURE 2. **Chemical *versus* enzymatic aggregation of Aβ.** *A*, glyceraldehyde-3-phosphate dehydrogenase (*G3PD*), aldolase (*Aldo*), and Aβ40 were treated with the chemical cross-linking reagent DMS or TGase and compared with untreated samples. All samples were incubated at 30 °C overnight, separated by SDS-PAGE, and stained with the protein dye, SYRPO Red. G3PD and Aldo could be readily cross-linked with DMS (*lanes 2* and *4*) but not with TGase (*lanes 8* and *10*). Conversely, Aβ was not cross-linked by DMS (*lane 6*) but formed aggregates in the presence of TGase (*lane 12*). *B* and *C*, the specificity of Aβ cross-linking was also assessed by SEC separation (Superdex 75 column, 2 M guanidine + 10 mM NaCl). Aβ treated with DMS showed no aggregation, as seen in *lane 6* of *panel A*. This material thus produced predominantly a monomeric peak at 27 min (*B*). Aβ aggregation occurred in the presence of TGase, as seen in *lane 12* of *panel A*. The SEC elution profile shows the transition from monomeric Aβ (27 min) to oligomeric Aβ (peaks at 24 min or earlier) (*C*). SDS-PAGE gels and SEC chromatograms show a single experiment but are representative of three separate experiments.

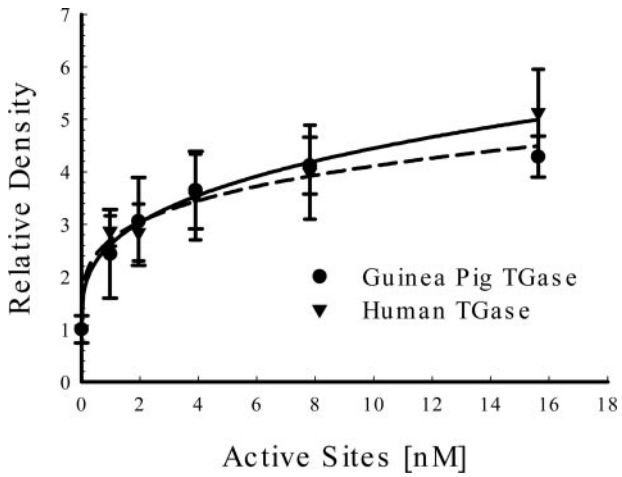

FIGURE 3. **Aggregation of Aβ40 induced by guinea pig and human TGase.** To directly compare the enzymatic activity of guinea pig and human TGase, the amount of catalytic sites in the two preparations was plotted against the substrate conversion as measured by densitometry of the Western blots (data not shown). The results showed that the two enzymes catalyze reactions with very similar kinetics ($n = 3$, ±S.E.).

residue in the mutant peptide, is available to react with TGase, as suggested by a weak 6E10 band near the molecular weight of TGase (76.6 kDa) (Fig. 1*F*, *lane 3*, *asterisk*). The presence of TGase in this band was confirmed by reprobing the same blot with anti-TGase antibodies (data not shown). These results suggest that TGase can specifically catalyze the oligomerization of Aβ40 and supports the previous finding that Aβ is a substrate for the enzyme (10–12).

To investigate the specificity of TGase-mediated cross-linking, we compared enzymatic with chemical cross-linking of Aβ. In Fig. 2*A*, cross-linking of three different substrates, glyceraldehyde-3-phosphate dehydrogenase (G3PD), aldolase, and Aβ, were compared. All proteins were separated using SDS-PAGE and visualized using SYPRO Red dye. G3PD and aldolase have previously been shown to multimerize in the presence of DMS and were used as positive controls (18). The addition of DMS to either protein induced higher molecular weight assemblies (Fig. 2*A*, *lanes 2* and *4*). In contrast, little to no oligomerization was observed with Aβ incubated with DMS (Fig. 2*A*, *lane 6*). Similar results were observed with all three proteins using the chemical cross-linker dimethyl adipimidate (data not shown). The finding that TGase induces robust oligomerization of Aβ (Fig. 2*A*, *lane 12*) but fails to cross-link G3PD or aldolase (Fig. 2*A*, *lanes 7–10*) suggests that cross-linking of Aβ by TGase is a specific reaction. Similar results were obtained when Aβ cross-linking was analyzed by SEC. Aβ treated with DMS and separated in 2 M guanidine HCl (to disassemble non-cross-linked Aβ) showed predominately monomeric Aβ (Fig. 2*B*). However, Aβ treated with TGase showed numerous peaks between 15 and 24 min (Fig. 2*C*), that presumably represent the dimeric, trimeric, and tetrameric Aβ assemblies observed on the Western blots. These data thus support the notion that TGase interacts with Aβ in a specific manner to promote oligomerization.

Because AD is specific to humans, a comparison was conducted between guinea pig and human TGase to validate the possibility of a role for this enzyme in the disease. Analysis of mouse and human TGase with calculated molecular weights of 76,699 and 77,253, respectively, showed an 84% homology at the protein level (25). Moreover, the active catalytic site is highly conserved in TGases from invertebrates to humans (26). Accordingly, a series of reactions conducted using guinea pig and human TGase showed similar oligomerization patterns by Western blotting (data not shown).

The molarity of the active sites was determined for the human and the guinea pig preparations according to Case and Stein (16) and was found to be 13.5 μM and 40 μM, respectively. The amount of oligomerization observed by Western blotting (data not shown) was plotted against the amount of catalytic activity for both guinea pig (*circles*) and human (triangles) TGase (Fig. 3). The results show that Aβ is an equally good substrate for both the human and guinea pig transglutaminase. This conclusion is further supported by the almost identical enzymatic activity previously observed for these two enzymes (16, 27).

To further study the potential role of TGase in AD, experiments were conducted to determine if another important, disease-related Aβ species, Aβ42, is also a substrate for TGase.

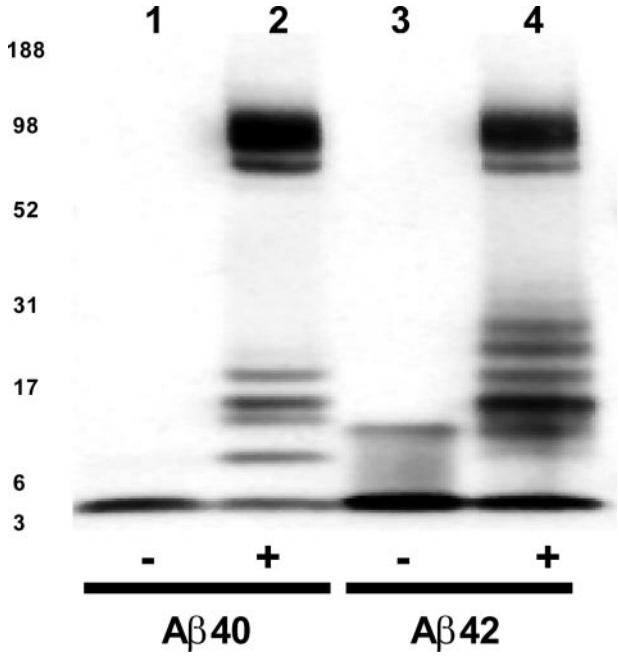

FIGURE 4. **Both Aβ40 and Aβ42 are substrates for TGase.** Aβ40 and Aβ42 were compared for their potential to serve as substrate for TGase. Aβ40 and Aβ42 were initially denatured in guanidine HCl and purified by SEC before the addition of TGase. Aβ40 and Aβ42 samples (7.5 μM each) incubated without TGase are shown in *lanes 1* and *3*, respectively, whereas Aβ40 and Aβ42 incubated with TGase are shown in *lanes 2* and *4*. The Western blot shown is representative of three separate experiments.

The possibility of Aβ42 being more pertinent to the pathophysiology of AD has been discussed, both because of its greater production relative to Aβ40 associated with familial AD mutations and because of its greater propensity to aggregate (28). The monomer is the predominant form of Aβ peptides observed without TGase (Fig. 4, *lanes 1* and *3*), with Aβ42 showing a slight tendency for self-assembly (Fig. 4, *lane 3*). In contrast, SDS-PAGE and immunoblotting showed oligomeric laddering for both Aβ40 and Aβ42 in the presence of TGase (Fig. 4, *lanes 2* and *4*). Even though TGase induced both peptides to rapidly oligomerize, there is a qualitative difference in the banding patterns representing the smaller oligomeric species (Fig. 4, *lane 2 versus 4*), whereas the high molecular weight bands appeared identical. This difference may relate to Aβ40 and Aβ42 being assembled through different pathways (29). Nonetheless, these results demonstrate that TGase recognizes both Aβ42 and Aβ40 as substrates.

To assess whether TGase catalyzes Aβ oligomerization at physiological Aβ concentrations, experiments were conducted with Aβ40 concentrations from the low nanomolar to the low micromolar range (Fig. 5). It was possible to detect TGase-induced oligomers of Aβ by our standard Western blotting procedure at Aβ concentrations of 500 and 1000 nM (Fig. 5*A*, *lane 3* and *4*, respectively), ~10- to 20-fold lower than the concentrations needed for Aβ self-assembly to normally occur (Fig. 5*A*, *lane 1*, no TGase). *Lane 2* contains only TGase, showing that the bands in *lanes 1*, *3*, and *4* were specific to Aβ and not due to the presence of TGase. TGase-induced oligomerization of Aβ may occur at even lower concentrations, but at Aβ concentrations below 500 nM protein bands were difficult to detect by Western blotting.

To determine whether TGase-induced oligomerization of Aβ could occur near physiological conditions, the Aβ40 concentration was lowered to 50 nM, but the reaction volume was increased to accommodate subsequent concentration of the sample to a level that was detectable by Western blotting. Aβ40 was incubated for 24 h with and without TGase (1.1×10^{-3} units/ml). The reactions were stopped with a final concentration of 50 mM EDTA and 0.11 mM SDS. SDS was critical for recovering low concentrations of Aβ by reducing Aβ loss due to binding to surfaces. The samples were then concentrated 1000-fold by spin filtration using a 3-kDa cutoff filter, limiting the loss of monomeric Aβ. After concentrating, samples were boiled to dissociate non-cross-linked oligomers formed by self-aggregation during the concentration process. Western blotting revealed that Aβ assemblies occurred only in the presence (Fig. 5*B*, *lane 2*) but not in the absence of TGase (Fig. 5*B*, *lane 1*). Bands could be detected in the sample containing TGase (see *arrows* in Fig. 2*B*, ~8 and 12 kDa) that were not present in the sample without TGase (*i.e.* 12-kDa band) or only in lower amounts (*i.e.* 8-kDa band) (Fig. 2*B*, *lane 1*). An additional large smear centered near 76 kDa (*asterisk*) was present in the concentrated sample containing TGase (Fig. 5*B*, *lane 2*), which was identified as TGase by anti-TGase antibodies in samples containing TGase and Aβ (Fig. 5*C*, *lane 2*) or TGase alone (Fig. 5*C*, *lane 3*). In these reactions TGase was not lowered proportionally to the decrease in Aβ, producing a higher molar ratio of TGase to Aβ than in standard reactions, thus explaining the prominent TGase bands on the Western blot after concentrating the samples. These high molecular weight bands also appeared in lanes containing Aβ and TGase developed with the anti-Aβ antibody (Fig. 5*B*, *lane 2*), but not in lanes containing only Aβ or only TGase (Fig. 5*B*, *lanes 1* and *3*, respectively), indicating that Aβ was bound to TGase. The formation of the 8-kDa, 12-kDa, and high molecular weight bands was compared in samples containing only Aβ and Aβ treated with TGase and quantified in Fig. 5*D*. These experiments indicate that TGase can induce Aβ oligomerization at physiologically relevant Aβ concentrations.

We used EM to visualize the TGase-induced Aβ assemblies, allowing for a comparison with previous EM studies of self-aggregating synthetic Aβ (14, 23, 30, 31). Aβ40 was denatured and purified by SEC prior to the addition of TGase. No structures were observed with fresh, SEC purified Aβ (data not shown). In Fig. 6, SEC purified Aβ (17 μM) was incubated with TGase (4×10^{-3} units/ml) at 30 °C for the times specified in the panels (2.5 min to 68 h). Very few structures were observed before 10–20 min, except for an occasional spherical particle of ~12 nm in diameter that was also seen in the sample containing only TGase (Fig. 6*K*). Western blot analysis suggested that smaller Aβ assemblies are present in the sample at time points before 10 min, but they seem to be too small to be visualized by EM (Fig. 6, *A–C*). After 10 min, structures appeared to be forming but were still too small to be clearly identified in EM images. Approximately 20 min after addition of TGase to Aβ, 5 nm spherical structures appeared (Fig. 6*D*). The exact time when these structures began to occur varied from experiment to experiment, but the observed morphologies of the Aβ species and their progression (Fig. 6, *A–E* and *G–I*) were consistent. By

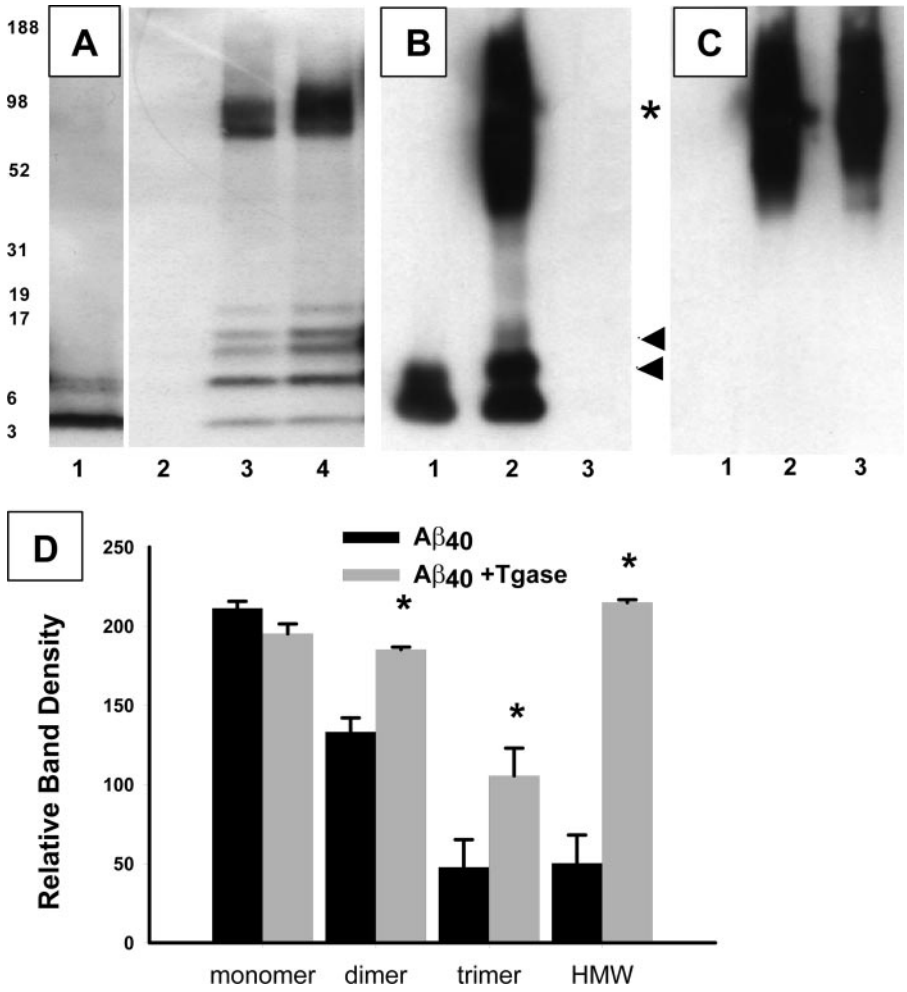

FIGURE 5. **TGase lowers the concentration of Aβ needed for aggregation.** *A*, *lanes 1* and *2* show control experiments containing either only Aβ40 or only TGase, respectively. Incubation of 0.5 μM (*lane 3*) or 1 μM (*lane 4*) Aβ with TGase caused aggregation. *B*, reactions were performed (24 h at room temperature) with an Aβ40 concentration of 50 nM without (*lane 1*) or with (*lane 2*) TGase (1.1×10^{-3} units/ml) and then stopped with EDTA and concentrated 1000-fold. In the presence of TGase, bands were observed at 8 and 12 kDa, indicating the formation of Aβ oligomers (*lane 2*, *arrows*). In the "*Aβ only*" sample (*lane 1*), the 12-kDa band was absent and the 8-kDa band was much less prominent. No bands were observed with the "*TGase only*" sample (*lane 3*). *C*, the same reaction as in *B* probed with an anti-TGase antibody revealed a large smear (*lane 2*, *asterisk*) similar to the heavy material seen in the immunoblot probed for Aβ (*panel B*, *lane 2*, *asterisk*). The sample in *lane 1* contains only Aβ and no TGase. Western blots are from a single experiment and are representative of a set of three to four separate experiments. *D*, Western blots ($n = 3$) as the one shown in *panel B* were quantified by densitometry. *, statistical significance at the $p < 0.05$ level using a paired *t* test comparing specific molecular weight bands in the Aβ + TGase sample with the corresponding bands in the Aβ only sample.

identical, to structures formed through self-assembly when Aβ reaches a critical concentration.

In support of the EM data, profiles of self-assembled *versus* TGase-induced Aβ species were compared by SEC in a non-denaturing buffer to determine if they had similar chromatographic profiles. Incubation of Aβ42 without TGase for 0, 6, or 16 h showed an SEC aggregation pattern almost identical to Aβ40 incubated with TGase for 0, 1, or 2 h (supplemental Fig. S1, *A* and *B*). The similarity of the formed aggregates was corroborated by the degree of β-sheet content of both preparations as measured by thioflavin T binding (supplemental Fig. S1*C*). Aβ40 incubated for 2 h without TGase showed no oligomerization and was identical to the 0-h profile (data not shown). The EM, SEC, and thioflavin T analyses support that TGase can induce Aβ oligomerization and aggregation in a manner similar to that observed with Aβ self-assembly.

Both neprilysin (NEP) and insulin-degrading enzyme (IDE) are thought to be important proteases involved in the degradation of Aβ *in vivo* (32–34). Clearly, these proteases degrade monomeric Aβ (35–37), but it is controversial whether these enzymes also degrade oligomeric Aβ species (38–41). Because AD pathology is thought not only to be due to an increase in Aβ aggregation but also to a failure of the body to degrade Aβ (42), the degradation of the TGase-induced Aβ polymers by these proteases was assessed.

30 min, the particles began to elongate, showing Aβ species that were ~6–8 nm in width, and up to 28 nm in length (Fig. 6*E*). The elongation continued with time (Fig. 6, *G–I*), whereas the width remained at ~6–8 nm. The structures that formed in the presence of TGase were almost identical to the previously described protofibrils that formed during self-assembly of synthetic Aβ40 incubated for 68 h at room temperature but at a concentration ~25 times greater (500 μM) (14, 23, 30, 31). The *inset* in Fig. 6*L* shows the heterogeneous size distribution of the formed protofibrils. The formation of these Aβ protofibrils was not due to self-assembly, because omission of calcium from the Aβ + TGase mixture prevented the aggregation (Fig. 6*F*), and Aβ40 incubated for 68 h in the absence of TGase also showed no aggregates (Fig. 6*J*). These experiments indicate that TGase can induce Aβ40 to form assemblies that are similar, if not

Incubation of SEC-purified, monomeric Aβ40 with TGase induced significant oligomerization (Fig. 7*A*, *lane 2*), which was inhibited by 10 μM TGase inhibitor LDDN-80042 (Fig. 7*A*, *lane 1*). In a third condition, the Aβ + TGase reaction was stopped after 0.5 h with 10 μM LDDN-80042 and then treated with 100 nM IDE at 37 °C for 30 min (Fig. 7*A*, *lane 3*). Although a large fraction of the monomer was degraded in the presence of IDE, no significant degradation was observed for the upper oligomeric Aβ bands (compare Fig. 7*A*, *lanes 2* and *3*). These changes were quantified by densitometry of the individual bands on a Western blot (Fig. 7*B*). Individual bands were normalized to their corresponding partner in the Aβ + TGase samples containing no IDE (*i.e.* no degradation was given a value of 1). A 60% loss of the monomer (4 kDa) was measured, whereas no degradation was observed for the bands containing

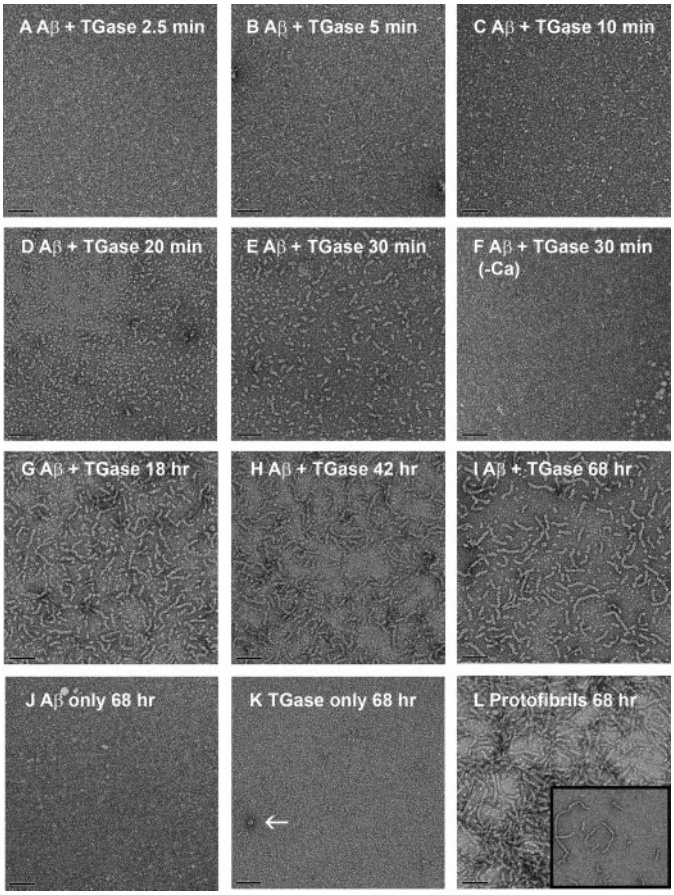

FIGURE 6. **TGase-induced aggregation produces defined Aβ assemblies.** Aβ40 was denatured with guanidine HCl, purified by SEC, incubated with TGase for 2.5 min to 68 h, and imaged by EM. No structures were observed at 2.5 or 5 min (*A* and *B*), but *spherical structures* became visible between 10 and 20 min (*C* and *D*). These particles became more elongated by 30 min (*E*) and grew further in length with time (*G–I*). In contrast, no structures were observed at 68 h with Aβ40 only (*J*) or TGase only (*K*) samples (except for an occasional 12 nm structure, presumably representing aggregates of TGase). The formation of the observed structures required TGase, because removal of calcium prevented their formation (*F*). TGase-induced Aβ assemblies are very similar to Aβ protofibrils formed by self-aggregation (500 μM, 68 h) (*L* and *inset*). *Images* are from a single time course experiment. The experiment was repeated three times resulting in identical Aβ structures, but the time when Aβ structures appeared varied between experiments as previously observed in the Western blot experiments. *Scale bars* represent 50 nm.

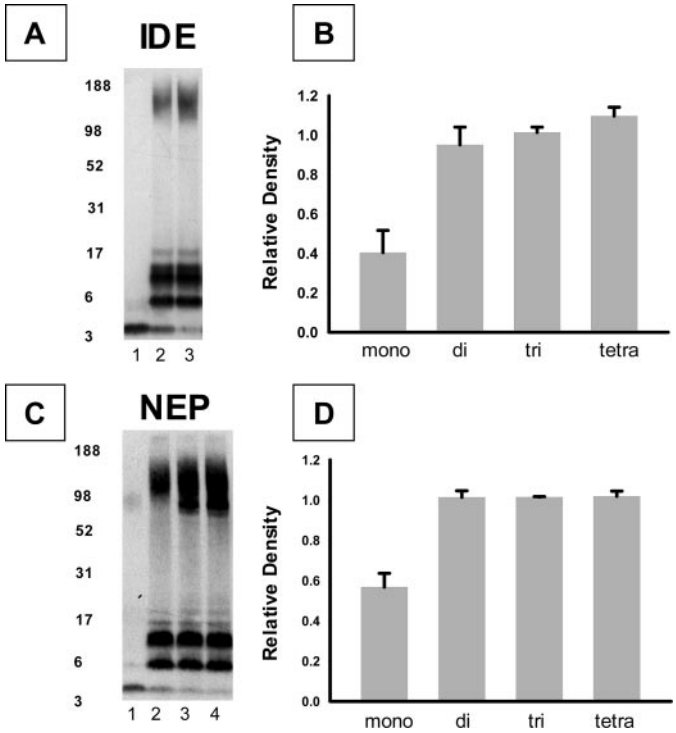

FIGURE 7. **TGase-induced Aβ aggregates are resistant to the proteases insulin degrading enzyme (IDE) and neprilysin (NEP).** *A*, Aβ was incubated with TGase, and the reaction was stopped with the TGase inhibitor LDDN-80042. Aβ aggregation did not occur when the TGase inhibitor was added at the beginning of the reaction (*lane 1*). TGase-treated Aβ samples were incubated without (*lane 2*) or with IDE (50 nM) (*lane 3*) showing little degradation of the oligomeric bands (>6 kDa). In contrast, monomeric Aβ (~4 kDa) remaining in the TGase-treated samples was susceptible to degradation by IDE (*lane 3*). *B*, quantitative analysis of the Western blots by densitometry showed a degradation of the monomer (*mono*) and no degradation of the oligomeric species. Each individual band in the IDE-treated sample (*lane 3*) was normalized to the signal of the corresponding band in the Aβ40 + TGase sample without IDE (*lane 2*). The bands in *lane 2* (*no IDE*) were given a value of 1. Each *bar* in the *graph* represents the mean of four or five individual experiments (±S.E.). *C*, NEP also degraded monomeric, but not oligomeric Aβ. No aggregation was observed if the inhibitor was added prior to TGase being added to Aβ (*lane 1*). NEP (38 and 76 nM) was added to TGase-treated Aβ (*lanes 3* and *4*, respectively) and showed degradation of monomeric, but not the oligomeric Aβ species (6 > kDa). *D*, by densitometry, a decrease in monomeric Aβ (~4 kDa) was observed in the presence of 76 nM NEP, whereas the 8-, 12-, and 16-kDa bands were not affected. *Bars* represent the mean of three individual experiments (±S.E.).

the 8-, 12-, or 16-kDa Aβ40 species ($n = 4–5$ for all conditions). These results suggest that IDE does not efficiently degrade TGase-induced Aβ40 oligomers.

Similar results were obtained for NEP, another protease thought to play a role in Aβ degradation. After halting the Aβ + TGase reaction by adding 10 μM TGase inhibitor LDDN-80042, the resulting Aβ oligomers were subjected to 38 and 76 nM NEP for 1 h at 37 °C (Fig. 7*C*, *lanes 3* and *4*, respectively). The ability of LDDN-80042 to inhibit TGase activity is seen in *lane 1* of Fig. 7*C* (compare Fig. 7*C*, *lane 1* (with inhibitor) with *lane 2* (without inhibitor)). Densitometry of the Western blot shows that monomeric Aβ40 was readily degraded (43% loss) (Fig. 7*D*, "*mono*"). Degradation of monomeric Aβ by NEP was completely blocked by 1 mM 1,10-phenanthroline (data not shown). Again, as with IDE, the Aβ assemblies generated by TGase were not significantly affected by NEP (8-, 12-, and 16-kDa bands in Fig. 7*D*). Thus, in both the NEP and IDE degradation assays, TGase-induced Aβ oligomers persisted despite significant degradation of monomeric Aβ by these proteases.

Various assemblies of both synthetic and biologically derived Aβ have been shown to inhibit LTP (43, 44), a cellular correlate to memory and learning (45). Using a well studied *N*-methyl-D-aspartate receptor-dependent paradigm (20), we tested whether TGase-induced Aβ assemblies would alter hippocampal LTP at the Schaffer collaterals-CA1 synapses. We produced Aβ assemblies with TGase, inhibiting the TGase reaction with LDDN-80042 (the resulting Aβ40 assemblies are shown in Fig. 8*D*) and then diluting the solution to 100 nM. LTP was induced in hippocampal slices from 26- to 35-day-old mice by two high frequency stimulations. LTP was significantly reduced by exposure of the hippocampal slices to 100 nM TGase-treated Aβ compared with ACSF or 100 nM Aβ receiving no TGase treatment (Fig. 8, *A–C*) (fEPSP slopes: Aβ + TGase = 107.7 ± 3.3%, $n = 14$, *versus* ACSF = 140.1 ± 3.7%, $n = 19$ or Aβ alone =

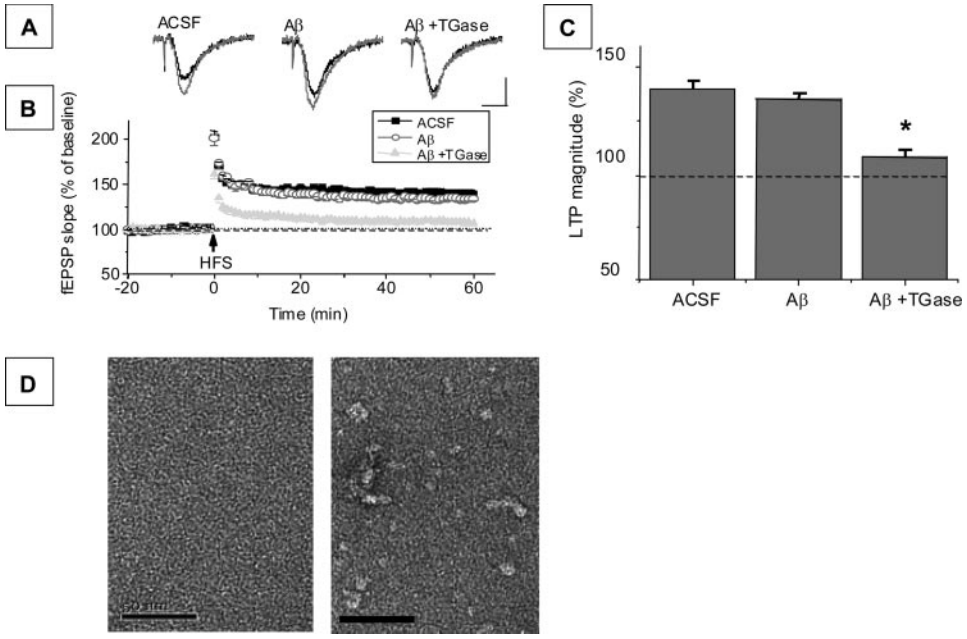

FIGURE 8. **TGase-treated Aβ inhibits LTP in the CA1 region of the hippocampus.** Aβ40 was incubated with or without TGase, and the reaction was stopped with the TGase inhibitor LDDN-80042. Aβ was diluted to 100 nM in ACSF, circulated over the slice for 30 min, and replaced with fresh ACSF containing no Aβ before tetanus. *A*, *traces* show typical fEPSPs elicited 5 min before (*black trace*) and 40 min after (*light gray trace*) high frequency stimulation (*horizontal calibration line* = 10 ms; *vertical line* = 0.5 mV). *B*, graph shows the plotting of the slope of the fEPSP for an individual experiment. High frequency stimulation (*arrow*) was used to induce LTP in hippocampal slices. The recorded fEPSP slope was plotted for three groups, ACSF only (*black solid boxes*), Aβ only (*open circles*), and Aβ + TGase (*light gray solid triangles*). *C*, data were summarized and graphed for LTP magnitudes from the three groups in *part B*. Data were pooled from slices of the same treatment group, and are presented as the mean ± S.E. (n = 14–15). Values expressed here represent 60-min time points after the conditioning stimulus. The Aβ + TGase condition was found to be statistically different from either the ACSF or Aβ treatment groups (*, $p < 0.001$, analysis of variance/Newman-Keuls post-hoc test). *D*, electron micrographs of untreated Aβ (*left image*) and TGase-treated Aβ (*right image*) show protofibril-like structures in the TGase-treated Aβ sample that inhibited LTP (*bar* = 100 nm).

134.9 ± 2.9%, $n = 15$, $p < 0.001$). Quantification shows that the TGase-induced Aβ assemblies produced a 76% decrease in LTP (Fig. 8*C*). The addition of TGase + LDDN-80042 (1 nM) or Aβ40 (100 nM) + LDDN-80042 (1 nM) had no effect on LTP, 153.4 ± 5.5% ($n = 3$) and 141.3 ± 4.9% ($n = 3$), respectively, compared with ACSF ($p > 0.05$). Our data would thus support the concept that TGase has not only the ability to lower the threshold for Aβ to assemble but it can also generate biologically active Aβ species that impair LTP.

DISCUSSION

Growing evidence implicates Aβ oligomerization and fibrillogenesis in the etiology of AD. However, *in vitro* models of fibrillogenesis by self-aggregation (3) require Aβ concentrations significantly higher than physiological concentrations (4–6). To date, there has been no successful attempt to reconcile this fact with the known presence of aggregated Aβ in patients with AD. The results presented here suggest that TGase catalyzes the oligomerization of Aβ at physiological concentrations and produces assemblies with morphologies similar to previously described protofibrils (14, 23), which have potential pathophysiological properties.

TGase has been suggested as playing a role in certain neurodegenerative diseases (8, 9). Multiple disease-associated substrates have been shown to be cross-linked by TGase: huntingtin in Huntington disease (46), ataxin-1 in spinocerebellar ataxia-1 (47), and Tau and Aβ in AD (48). There is additional support for the involvement of TGase in AD. First, TGase occurs abundantly in the brain, especially in areas thought to be affected by AD (49). Second, increased concentrations and higher activity of TGase have been found in AD patients relative to age-matched controls (49–52). Third, a splice variant found only in AD tissue produces a truncated form of the enzyme, which lacks the calcium regulatory domain of the full-length enzyme (53). Fourth, the identification of the ε-*N*-(γ-glutamyl)lysine isopeptide bond specific to TGase activity in the cerebrospinal fluid has high sensitivity and selectivity for the diagnosis of AD (54). Finally, Aβ contains the necessary lysine and glutamine residues and has been shown to be a substrate for TGase (10–12). This particular feature of Aβ, combined with the many associations between TGase and AD, suggests that TGase could be an effective facilitator of Aβ oligomerization *in vivo*.

An important aspect of the results presented here is the observation that TGase can lower the oligomerization threshold from the high concentrations needed for *in vitro* self-assembly to nanomolar concentrations, approaching physiological concentrations found in AD brain tissue (4–6). Western blot analysis of TGase reactions conducted with Aβ concentrations as low as 50 nM shows the formation of Aβ oligomers. These structures survive boiling in SDS, suggesting that they are not due to concentrating the sample, but are stabilized by covalent bonds. The immunoblot results showed the formation of 6E10-immunoreactive material in a band located between ~40 and 180 kDa. This "smeared" banding pattern contains TGase (76 kDa), suggesting that Aβ oligomers of varying lengths are cross-linked to TGase. The prominence of this smear is due to the concentrating of the TGase, which is retained by the 3-kDa spin filter used to concentrate the Aβ assemblies. If Aβ-TGase bonds were being exclusively catalyzed, the immunoblot results would show only distinct bands around the molecular weight of TGase or above. However, specific oligomeric Aβ-Aβ bands (lower than the molecular weight of TGase) were also observed, specifically the formation of 8- and 12-kDa bands, which were not present or in lower concentrations than in the concentrated samples containing only Aβ. Higher order intermediates may be forming under these conditions, but may not be detected due to their low concentrations and possible loss during the concentration step. Additionally, it is possible that the TGase-Aβ

interaction is affecting the catalytic activity of TGase (*i.e.* is poisoning the enzyme) or is removing Aβ from the reaction by its binding to TGase. Nonetheless, our data suggest that the formation of these Aβ-specific reaction products at low nanomolar concentrations is catalyzed by TGase, thus lowering the threshold for oligomerization by a factor of 100 or more.

Our studies show that TGase not only stabilizes these structures but allows Aβ to assemble into structures that are similar to those observed upon self-aggregation. A number of soluble Aβ morphologies have been imaged and investigated: Aβ oligomers, Aβ-derived diffusible ligands, amylospheroids, pores, and protofibrils (38, 44, 55–61). Protofibrils form through an orderly process, visually starting as small, 5–6 nm globular structures, which appear to coalesce into longer and longer curvilinear structures that ultimately form fibrils (14, 29, 30, 62) (also see Ref. 63). From the EM images presented here, Aβ aggregates induced by TGase transition through almost identical intermediates as those observed with protofibrils. In support of this observation, binding of Thioflavin T to TGase-induced Aβ aggregates was very similar to its binding to self-aggregated Aβ42, indicating similar formation of β-sheet structures (see supplemental data). These data would suggest that TGase is inducing oligomerization and aggregation in Aβ in a specific manner, catalyzing pathogenic folding in a manner similar to self-assembly.

Similar to the data presented here for Aβ, previous studies have found that TGase can induce the oligomerization and aggregation of various proteins, including Aβ, α-synuclein, huntingtin, and Tau (10, 11, 64–66). However, other studies have shown that TGase can also inhibit protein aggregation, which was illustrated with some of the same proteins, including Tau, α-synuclein, and huntingtin, but also for truncated yeast prion Sup35 and β-lactoglobulin (67–69). The effect of TGase cross-linking, promotion *versus* inhibition of protein aggregation, may be determined by whether TGase catalyzes the formation of cross-links within a protein, which could inhibit aggregation, or between two proteins, which could enhance aggregation. Because cross-linking by TGase requires a glutamine and a lysine residue, the degree of intra- *versus* intermolecular cross-linking may depend on the position of these two amino acids relative to each other in the folded protein. A mutational analysis of the two lysines in Aβ showed that only substitution of Lys-16 inhibited aggregation, whereas mutating Lys-28 had no effect (10), suggesting that only Lys-16 plays a role in Aβ aggregation. The only Gln residue in Aβ is Gln-15, directly preceding Lys-16. There are currently no data that address the question whether intramolecular cross-links can form between the adjacent amino acids Gln-15 and Lys-16. Our observation that TGase induces oligomerization of Aβ would, however, favor the notion that TGase catalyzes the formation of intermolecular cross-links between Gln-15 in one Aβ monomer with Lys-16 in a second Aβ monomer. Although intramolecular cross-linking between Gln-15 and Lys-16 would also compete with the formation of intermolecular cross-links, the fact that we see TGase-induced oligomerization of Aβ argues against significant formation of intramolecular cross-links.

According to a model of the Aβ structure (70), Gln-15 and Lys-16 would be immediately adjacent to a hydrophobic region critical for aggregation of Aβ (71). The effect of TGase-catalyzed formation of intermolecular cross-links between Aβ subunits might be that the hydrophobic regions are brought into close proximity, thus enhancing oligomerization, especially at low Aβ concentrations. Konno *et al.* (67, 68) suggested that the concentration of the substrate may determine the prevalence of intra- *versus* intermolecular cross-linking, with low concentrations favoring intramolecular cross-links, which in turn are thought to inhibit oligomerization and/or aggregation. Our studies show, however, that TGase can induce oligomerization even at low, nanomolar concentrations of Aβ. Furthermore, pre-existing self-assembled Aβ oligomers would be a much better substrate for TGase, because the Gln and Lys residues from different monomers would already be pre-oriented for cross-linking. However, even our monomeric Aβ preparation (*i.e.* purified by SEC in 6 M guanidine HCl) was a good substrate for TGase to induce the formation of oligomers protofibrils. Our data thus suggest that TGase favors to catalyze intermolecular cross-links, inducing the formation of Aβ oligomers, but we cannot rule out the possibility that intramolecular cross-linking is also occurring. It is possible that intramolecular cross-linking is competing with intermolecular cross-linking and slows down the oligomerization process we observe. How the abnormal folding of Aβ is initiated in AD is unknown, but possibly TGase may determine the degree to which Aβ folding is directed toward a pathogenic rather than non-pathogenic pathway. The transition from monomer to fibril is a complex process, and recent data showed that cross-linking with 4-hydroxynoneal enhanced oligomerization but blocked fibrillogenesis (72). Of further interest is the recent finding that various chemical compounds can separate the oligomerization and fibrillogenesis pathways (73). These findings will be important in determining which pathway is critical for the pathogenesis of AD and will help shape the therapeutic strategy that should be used to block the pathogenic Aβ assembly process.

In addition to Aβ aggregation, the time-dependent accumulation of Aβ in the brain is another invariable component observed in AD. Proposed mechanisms for the pathological accumulation of Aβ include not only the formation of Aβ aggregates but also an inability of the body to degrade Aβ. Thus, mechanisms describing the failure of Aβ being degraded are also vital to understanding the initial pathogenic accumulation of Aβ. Here, we show that the TGase-induced oligomeric Aβ species are resistant to both NEP and IDE, two proteases thought to be important for Aβ degradation *in vivo* (42), whereas the monomer was readily degraded by both metalloproteases. The importance of these results is corroborated by the manipulation of these proteases in animal models showing that increasing or decreasing their activity can alter Aβ accumulation inversely (74) as well as change synaptic function and behavior (75, 76). Therefore, initiating Aβ aggregation could cause the incapacitation of these proteases by allowing Aβ to aggregate before the monomer can be proteolytically degraded. Our findings suggest that, once Aβ assemblies have formed due to TGase activity, they should persist *in vivo*, resulting in a progressive buildup of Aβ. Should these Aβ assemblies be physiologically active, this persistence could increase their contribu-

tion to the progressive neurodegeneration process observed in AD.

In associating Aβ species with pathology, soluble forms of aggregated Aβ correlate best with synaptic loss (77) and histopathological changes (78). These synaptic changes have been predictive of cognitive decline (79). Further support is provided by the findings that soluble forms of Aβ can specifically bind and disrupt synapses (61, 80, 81, 83). Additionally, previous studies have shown that Aβ assemblies can mimic some of the symptomatology of AD, including alterations in synaptic function, memory and learning, and behavior, suggesting their early involvement in the progression of AD (38, 44, 55, 56, 84–89). In support of TGase catalyzing the formation of potentially pathological species of Aβ, we observed that Aβ40 treated with TGase inhibited LTP at 100 nM Aβ40, but not when Aβ or TGase were applied individually. These data are consistent with previous studies showing that various preparations of aggregated Aβ can inhibit LTP (38, 44, 55, 82, 84, 87–89).

The data presented here have physiological importance, because our results show that TGase may contribute to important attributes observed in AD: 1) TGase can initiate aggregation at physiological Aβ concentrations. TGase may not have to cross-link a large percentage of Aβ molecules to play a role in aggregation but may be important in driving the oligomerization or nucleating the aggregation process, allowing the self-aggregation to proceed more efficiently (3, 11); 2) TGase can cause the accumulation of soluble Aβ species by producing protease-resistant Aβ assemblies; and 3) the Aβ species induced by TGase can inhibit processes involved in learning and memory, one of the first clinical symptoms observed in AD. For these reasons TGase may play an important role in the initiation and progression of AD. Therefore, the pharmacological manipulation of TGase could be a therapeutic strategy for slowing or blocking the progress of AD.

Acknowledgments—We thank the members of the Laboratory of Neurodegeneration and Drug Discovery, Partners Healthcare, Dr. Ross Stein, April Case, and Dr. Greg Cuny for helpful discussions and the gift of the TGase inhibitor LDDN-80042 and human TGase. We thank Dr. Malcolm Leissring for his intellectual contributions and the gift of IDE. We thank Drs. Hilal Lashuel and David Teplow for insightful discussions. The molecular EM facility at Harvard Medical School was established with a generous donation from the Giovanni Armenise Harvard Center for Structural Biology and is maintained with funds from National Institutes of Health Grant GM62580 (to T. W.). We thank B. Hartley for editorial assistance.

REFERENCES

1. Jarrett, J. T., Berger, E. P., and Lansbury, P. T., Jr. (1993) *Biochemistry* **32,** 4693–4697
2. Pike, C. J., Burdick, D., Walencewicz, A. J., Glabe, C. G., and Cotman, C. W. (1993) *J. Neurosci.* **13,** 1676–1687
3. Harper, J. D., and Lansbury, P. T. (1997) *Annu. Rev. Biochem.* **66,** 385–407
4. Fagan, A. M., Mintun, M. A., Mach, R. H., Lee, S. Y., Dence, C. S., Shah, A. R., LaRossa, G. N., Spinner, M. L., Klunk, W. E., Mathis, C. A., DeKosky, S. T., Morris, J. C., and Holtzman, D. M. (2006) *Ann. Neurol.* **59,** 512–519
5. Nitsch, R. M., Rebeck, G. W., Deng, M., Richardson, U. I., Tennis, M., Schenk, D. B., Vigo-Pelfrey, C., Lieberburg, I., Wurtman, R. J., Hyman, B. T., *et al.* (1995) *Ann. Neurol.* **37,** 512–518
6. Samuels, S. C., Silverman, J. M., Marin, D. B., Peskind, E. R., Younki, S. G., Greenberg, D. A., Schnur, E., Santoro, J., and Davis, K. L. (1999) *Neurology* **52,** 547–551
7. Griffin, M., Casadio, R., and Bergamini, C. M. (2002) *Biochem. J.* **368,** 377–396
8. Lesort, M., Tucholski, J., Miller, M. L., and Johnson, G. V. (2000) *Prog. Neurobiol.* **61,** 439–463
9. Citron, B. A., Zoloty, J. E., Suo, Z., and Festoff, B. W. (2005) *Brain Res. Mol. Brain Res.* **135,** 122–133
10. Ikura, K., Takahata, K., and Sasaki, R. (1993) *FEBS Lett.* **326,** 109–111
11. Dudek, S. M., and Johnson, G. V. W. (1994) *Brain Res.* **651,** 129–133
12. Wakshlag, J. J., Antonyak, M. A., Boehm, J. E., Boehm, K., and Cerione, R. A. (2006) *Protein J.* **25,** 83–94
13. Walsh, D. M., Hartley, D. M., Kusumoto, Y., Fezoui, Y., Condron, M. M., Lomakin, A., Benedek, G. B., Selkoe, D. J., and Teplow, D. B. (1999) *J. Biol. Chem.* **274,** 25945–25952
14. Walsh, D. M., Lomakin, A., Benedek, G. B., Maggio, J. E., Condron, M. M., and Teplow, D. B. (1997) *J. Biol. Chem.* **272,** 22364–22374
15. Conway, K. A., Harper, J. D., and Lansbury, P. T. (1998) *Nat. Med.* **4,** 1318–1320
16. Case, A., and Stein, R. L. (2003) *Biochemistry* **42,** 9466–9481
17. Piper, J. L., Gray, G. M., and Khosla, C. (2002) *Biochemistry* **41,** 386–393
18. Davies, G. E., and Stark, G. R. (1970) *Proc. Natl. Acad. Sci. U. S. A.* **66,** 651–656
19. Ohi, M., Li, Y., Cheng, Y., and Walz, T. (2004) *Biol. Proced. Online* **6,** 23–34
20. Li, S., Tian, X., Hartley, D. M., and Feig, L. A. (2006) *J. Neurosci.* **26,** 1721–1729
21. Anderson, W. W., and Collingridge, G. L. (2001) *J. Neurosci. Methods* **108,** 71–83
22. Lomakin, A., Chung, D. S., Benedek, G. B., Kirschner, D. A., and Teplow, D. A. (1996) *Proc. Natl. Acad. Sci. U. S. A.* **93,** 1125–1129
23. Harper, J. D., Wong, S. S., Lieber, C. M., and Lansbury, P. T. (1997) *Chem. Biol.* **4,** 119–125
24. Duval, E., Case, A., Stein, R. L., and Cuny, G. D. (2005) *Bioorg. Med. Chem. Lett.* **15,** 1885–1889
25. Gentile, V., Saydak, M., Chiocca, E. A., Akande, O., Birckbichler, P. J., Lee, K. N., Stein, J. P., and Davies, P. J. (1991) *J. Biol. Chem.* **266,** 478–483
26. Chen, J. S., and Mehta, K. (1999) *Int. J. Biochem. Cell Biol.* **31,** 817–836
27. Case, A., and Stein, R. L. (2007) *Biochemistry* **46,** 1106–1115
28. Lansbury, P. T., and Lashuel, H. A. (2006) *Nature* **443,** 774–779
29. Bitan, G., Kirkitadze, M. D., Lomakin, A., Vollers, S. S., Benedek, G. B., and Teplow, D. B. (2003) *Proc. Natl. Acad. Sci. U. S. A.* **100,** 330–335
30. Lashuel, H. A., Hartley, D. M., Petre, B. M., Wall, J. S., Simon, M. N., Walz, T., and Lansbury, J. P. T. (2003) *J. Mol. Biol.* 795–808
31. Goldsbury, C., Frey, P., Olivieri, V., Aebi, U., and Muller, S. A. (2005) *J. Mol. Biol.* **352,** 282–298
32. Leissring, M. A., Farris, W., Chang, A. Y., Walsh, D. M., Wu, X., Sun, X., Frosch, M. P., and Selkoe, D. J. (2003) *Neuron* **40,** 1087–1093
33. Iwata, N., Tsubuki, S., Takaki, Y., Watanabe, K., Sekiguchi, M., Hosoki, E., Kawashima-Morishima, M., Lee, H. J., Hama, E., Sekine-Aizawa, Y., and Saido, T. C. (2000) *Nat. Med.* **6,** 143–150
34. Kurochkin, I. V., and Goto, S. (1994) *FEBS Lett.* **345,** 33–37
35. Qiu, W. Q., Walsh, D. M., Ye, Z., Vekrellis, K., Zhang, J., Podlisny, M., Rosner, M. R., Safavi, A., Hersh, L. B., and Selkoe, D. J. (1998) *J. Biol. Chem.* **273,** 32730–32738
36. Vekrellis, K., Ye, Z., Qiu, W. Q., Walsh, D., Hartley, D., Chesneau, V., Rosner, M. R., and Selkoe, D. J. (2000) *J. Neurosci.* **20,** 1657–1665
37. Leissring, M. A., Lu, A., Condron, M. M., Teplow, D. B., Stein, R. L., Farris, W., and Selkoe, D. J. (2003) *J. Biol. Chem.* **278,** 37314–37320
38. Walsh, D. M., Klyubin, I., Fadeeva, J. V., Cullen, W. K., Anwyl, R., Wolfe, M. S., Rowan, M. J., and Selkoe, D. J. (2002) *Nature* **416,** 535–539
39. Kanemitsu, H., Tomiyama, T., and Mori, H. (2003) *Neurosci. Lett.* **350,** 113–116
40. Mazur-Kolecka, B., and Frackowiak, J. (2006) *Brain Res.* **1124,** 10–18
41. El-Amouri, S. S., Zhu, H., Yu, J., Gage, F. H., Verma, I. M., and Kindy, M. S. (2007) *Brain Res.* **1152,** 191–200
42. Tanzi, R. E., Moir, R. D., and Wagner, S. L. (2004) *Neuron* **43,** 605–608

43. Rowan, M. J., Klyubin, I., Wang, Q., and Anwyl, R. (2005) *Biochem. Soc. Transact.* **33,** 563–567
44. Lesne, S., Koh, M. T., Kotilinek, L., Kayed, R., Glabe, C. G., Yang, A., Gallagher, M., and Ashe, K. H. (2006) *Nature* **440,** 352–357
45. Cooke, S. F., and Bliss, T. V. (2006) *Brain* **129(Pt 7),** 1659–1673
46. Zainelli, G. M., Dudek, N. L., Ross, C. A., Kim, S. Y., and Muma, N. A. (2005) *J. Neuropathol. Exp. Neurol.* **64,** 58–65
47. D'Souza, D. R., Wei, J., Shao, Q., Hebert, M. D., Subramony, S. H., and Vig, P. J. (2006) *Neurosci. Lett.* **409,** 5–9
48. Muma, N. A. (2007) *J. Neuropathol. Exp. Neurol.* **66,** 258–263
49. Johnson, G. V., Cox, T. M., Lockhart, J. P., Zinnerman, M. D., Miller, M. L., and Powers, R. E. (1997) *Brain Res.* **751,** 323–329
50. Bonelli, R. M., Aschoff, A., Niederwieser, G., Heuberger, C., and Jirikowski, G. (2002) *Neurobiol. Dis.* **11,** 106–110
51. Kim, S. Y., Grant, P., Lee, J. H., Pant, H. C., and Steinert, P. M. (1999) *J. Biol. Chem.* **274,** 30715–30721
52. Zhang, W., Johnson, B. R., Suri, D. E., Martinez, J., and Bjornsson, T. D. (1998) *Acta Neuropathol.* (*Berl.*) **96,** 395–400
53. Citron, B. A., SantaCruz, K. S., Davies, P. J., and Festoff, B. W. (2001) *J. Biol. Chem.* **276,** 3295–3301
54. Nemes, Z., Fesus, L., Egerhazi, A., Keszthelyi, A., and Degrell, I. M. (2001) *Neurobiol. Aging* **22,** 403–406
55. Lambert, M. P., Barlow, A. K., Chromy, B. A., Edwards, C., Freed, R., Liosatos, M., Morgan, T. E., Rozovsky, I., Trommer, B., Viola, K. L., Wals, P., Zhang, C., Finch, C. E., Krafft, G. A., and Klein, W. L. (1998) *Proc. Natl. Acad. Sci. U. S. A.* **95,** 6448–6453
56. Hartley, D., Walsh, D. M., Ye, C. P., Diehl, T., Vasquez, S., Vassilev, P. M., Teplow, D. B., and Selkoe, D. J. (1999) *J. Neurosci.* **19,** 8876–8884
57. Kawahara, M., Kuroda, Y., Arispe, N., and Rojas, E. (2000) *J. Biol. Chem.* **275,** 14077–14083
58. Hoshi, M., Sato, M., Matsumoto, S., Noguchi, A., Yasutake, K., Yoshida, N., and Sato, K. (2003) *Proc. Natl. Acad. Sci. U. S. A.* **100,** 6370–6375
59. Lashuel, H. A., Hartley, D., Petre, B. M., Walz, T., and Lansbury, P. T. (2002) *Nature* **418,** 291
60. Quist, A., Doudevski, I., Lin, H., Azimova, R., Ng, D., Frangione, B., Kagan, B., Ghiso, J., and Lal, R. (2005) *Proc. Natl. Acad. Sci. U. S. A.* **102,** 10427–10432
61. Whalen, B. M., Selkoe, D. J., and Hartley, D. M. (2005) *Neurobiol. Dis.* **20,** 254–266
62. Harper, J. D., Lieber, C. M., and Lansbury, P. T. (1997) *Chem. Biol.* **4,** 951–959
63. Srinivasan, R., Jones, E. M., Liu, K., Ghiso, J., Marchant, R. E., and Zagorski, M. G. (2003) *J. Mol. Biol.* **333,** 1003–1023
64. Kahlem, P., Green, H., and Djian, P. (1998) *Mol. Cell* **1,** 595–601
65. Miller, M. L., and Johnson, G. V. (1995) *J. Neurochem.* **65,** 1760–1770
66. Junn, E., Ronchetti, R. D., Quezado, M. M., Kim, S. Y., and Mouradian, M. M. (2003) *Proc. Natl. Acad. Sci. U. S. A.* **100,** 2047–2052
67. Konno, T., Morii, T., Hirata, A., Sato, S., Oiki, S., and Ikura, K. (2005) *Biochemistry* **44,** 2072–2079
68. Konno, T., Morii, T., Shimizu, H., Oiki, S., and Ikura, K. (2005) *J. Biol. Chem.* **280,** 17520–17525
69. Karpuj, M. V., Garren, H., Slunt, H., Price, D. L., Gusella, J., Becher, M. W., and Steinman, L. (1999) *Proc. Natl. Acad. Sci. U. S. A.* **96,** 7388–7393
70. Urbanc, B., Cruz, L., Yun, S., Buldyrev, S. V., Bitan, G., Teplow, D. B., and Stanley, H. E. (2004) *Proc. Natl. Acad. Sci. U. S. A.* **101,** 17345–17350
71. Petkova, A. T., Ishii, Y., Balbach, J. J., Antzutkin, O. N., Leapman, R. D., Delaglio, F., and Tycko, R. (2002) *Proc. Natl. Acad. Sci. U. S. A.* **99,** 16742–16747
72. Siegel, S. J., Bieschke, J., Powers, E. T., and Kelly, J. W. (2007) *Biochemistry* **46,** 1503–1510
73. Necula, M., Kayed, R., Milton, S., and Glabe, C. G. (2007) *J. Biol. Chem.* **282,** 10311–10324
74. Eckman, E. A., and Eckman, C. B. (2005) *Biochem. Soc. Transact.* **33,** 1101–1105
75. Huang, S. M., Mouri, A., Kokubo, H., Nakajima, R., Suemoto, T., Higuchi, M., Staufenbiel, M., Noda, Y., Yamaguchi, H., Nabeshima, T., Saido, T. C., and Iwata, N. (2006) *J. Biol. Chem.* **281,** 17941–17951
76. Madani, R., Poirier, R., Wolfer, D. P., Welzl, H., Groscurth, P., Lipp, H. P., Lu, B., Mouedden, M. E., Mercken, M., Nitsch, R. M., and Mohajeri, M. H. (2006) *J. Neurosci. Res.* **84,** 1871–1878
77. Lue, L. F., Kuo, Y. M., Roher, A. E., Brachova, L., Shen, Y., Sue, L., Beach, T., Kurth, J. H., Rydel, R. E., and Rogers, J. (1999) *Am. J. Pathol.* **155,** 853–862
78. McLean, C. A., Cherny, R. A., Fraser, F. W., Fuller, S. J., Smith, M. J., Beyreuther, K., Bush, A. I., and Masters, C. L. (1999) *Ann. Neurol.* **46,** 860–866
79. Terry, R. D., Masliah, E., Salmon, D. P., Butters, N., DeTeresa, R., Hill, R., Hansen, L. A., and Katzman, R. (1991) *Ann. Neurol.* **30,** 572–580
80. Mucke, L., Masliah, E., Yu, G. Q., Mallory, M., Rockenstein, E. M., Tatsuno, G., Hu, K., Kholodenko, D., Johnson-Wood, K., and McConlogue, L. (2000) *J. Neurosci.* **20,** 4050–4058
81. Lacor, P. N., Buniel, M. C., Chang, L., Fernandez, S. J., Gong, Y., Viola, K. L., Lambert, M. P., Velasco, P. T., Bigio, E. H., Finch, C. E., Krafft, G. A., and Klein, W. L. (2004) *J. Neurosci.* **24,** 10191–10200
82. Townsend, M., Shankar, G. M., Mehta, T., Walsh, D. M., and Selkoe, D. J. (2006) *J. Physiol.* **572,** 477–492
83. Deshpande, A., Mina, E., Glabe, C., and Busciglio, J. (2006) *J. Neurosci.* **26,** 6011–6018
84. Wang, H. W., Pasternak, J. F., Kuo, H., Ristic, H., Lambert, M. P., Chromy, B., Viola, K. L., Klein, W. L., Stine, W. B., Krafft, G. A., and Trommer, B. L. (2002) *Brain Res.* **924,** 133–140
85. Ye, C. P., Selkoe, D. J., and Hartley, D. M. (2003) *Neurobiol. Dis.* **13,** 177–190
86. Ye, C., Walsh, D. M., Selkoe, D. J., and Hartley, D. M. (2004) *Neurosci. Lett.* **366,** 320–325
87. Wang, Q., Rowan, M. J., and Anwyl, R. (2004) *J. Neurosci.* **24,** 6049–6056
88. Klyubin, I., Walsh, D. M., Cullen, W. K., Fadeeva, J. V., Anwyl, R., Selkoe, D. J., and Rowan, M. J. (2004) *Eur. J. Neurosci.* **19,** 2839–2846
89. Walsh, D. M., Townsend, M., Podlisny, M. B., Shankar, G. M., Fadeeva, J. V., El Agnaf, O., Hartley, D. M., and Selkoe, D. J. (2005) *J. Neurosci.* **25,** 2455–2462